Research Article

A New Approach for Enhancing the Services of the 5G Mobile Network and IOT-Related Communication Devices Using Wavelet-OFDM and Its Applications in Healthcare

Mordecai F. Raji [ID],[1] **JianPing Li** [ID],[1] **Amin Ul Haq** [ID],[1] **Victor Ejianya** [ID],[2] **Jalaluddin Khan** [ID],[1] **Asif Khan** [ID],[1] **Mudassir Khalil** [ID],[1] **Amjad Ali** [ID],[3] **Ghufran A. khan** [ID],[4] **Mohammad Shahid** [ID],[5] **Bilal Ahamad** [ID],[6] **Amit Yadav** [ID],[7] and **Imran Memon** [ID][8]

[1]*School of Computer Science and Engineering, University of Electronic Science and Technology of China, Chengdu, China*
[2]*School of Computer and Information Engineering, Zhejiang Gongshang University, Hangzhou, China*
[3]*Department of Computer Science and Software Technology, University of Swat, Mingora, Pakistan*
[4]*School of Information Science and Technology, Southwest Jiaotong University, Chengdu, China*
[5]*Department of Computer Science and Information Engineering, National Taiwan University of Science and Technology, Taipei, Taiwan*
[6]*Department of Computer Science, Shaqra University, Shaqra, Saudi Arabia*
[7]*Department of Information Management, Chengdu Neusoft University, Chengdu, Sichuan, China*
[8]*Department of Computer Science, Bahria University, Islamabad, Sindh, Pakistan*

Correspondence should be addressed to Mordecai F. Raji; mraji@qq.com, JianPing Li; jpli2222@uestc.edu.cn, Amin Ul Haq; khan.amin50@yahoo.com, and Asif Khan; asifkhan@uestc.edu.cn

The heart of the current wireless communication systems (including 5G) is the Fourier transform-based orthogonal frequency division multiplex (OFDM). Over time, a lot of research has proposed the wavelet transform-based OFDM as a better replacement of Fourier in the physical layer solutions because of its performance and ability to support network-intensive applications such as the Internet of Things (IoT). In this paper, we weigh the wavelet transform performances against the future wireless application system requirements and propose guidelines and approaches for wavelet applications in 5G waveform design. This is followed by a detailed impact on healthcare. Using an image as the test data, a comprehensive performance comparison between Fourier transform and various wavelet transforms has been done considering the following 5G key performance indicators (KPIs): energy efficiency, modulation and demodulation complexity, reliability, latency, spectral efficiency, effect of transmission/reception under asynchronous transmission, and robustness to time-/frequency-selective channels. Finally, the guidelines for wavelet transform use are presented. The guidelines are sufficient to serve as approaches for tradeoffs and also as the guide for further developments.

1. Introduction

The number of devices connected to the internet is on the increase. The advent of the IoT will make it an explosive one [1, 2]. Almost every 10 years, a new generation of wireless communication standard is developed to meet the exponentially growing demand for fast and reliable connections.

Wireless service consumers have experienced the growth and maturity of 2G, 3G, and 4G mobile network systems. Now, the International Telecommunication Union (ITU) has defined the expectations for 5G New Radio (NR). The 5G requirements are classified into enhanced mobile broadband (eMBB), ultrareliable low-latency communication (URLLC), and massive machine-type communication (mMTC). All

these classifications are subsets of IOT's requirements. Their requirements are not limited to multi-gigabit-per-second (Gbps) data rates, low latency, high spectral efficiency, high mobility, and high connection density [3]. We can, therefore, conclude that 5G will have to cope with a high degree of heterogeneity in terms of services and requirements. Surprisingly, the increasing number of certain new applications as well as newer, yet to be conceived applications, will require even greater data rates among other requirements than what 5G NR can offer [4], and some of those applications might not even fall completely within a single defined use-case [5]. A few of them are virtual/augmented reality (VR/AR), wireless cognition, and wireless backhaul. Furthermore, because of 5G's diversity, there possibly exist other undiscovered areas of applications such as in healthcare, of which IoT is obviously the enabler. Advances in a research area will impact the other; it is like a chain reaction; for example, 5G (as the underlying technology) will unlock IoT capabilities that were previously unattainable on 4G networks. It will introduce major innovations, such as higher connection speed, greater capacity, and lower latency. Over time, these benefits will lead to technological milestones that will have a significant impact on healthcare and other areas. Therefore, for an efficient IoT system, there is a need for a diverse network such as 5G. The advent of 5G has led to further exploration of new methodology, hardware, waveform design, underutilized millimeter-wave (mm-wave) frequency, etc. The most prominent of these explorations but most challenging would be to design waveform for efficient signaling in 5G. The summary of the proposed waveforms is given in [6].

OFDM remains the key ingredient in waveform design for many multicarrier wireless communication schemes [7]. Proposed waveforms for 5G are mostly OFDM-inspired. This reason is partly due to OFDM's use in 4G LTE and other standards, familiarity among the wireless society, and its maturity as a technology [8, 9]. However, the gradual migration from cell-centric to user-centric processing is rendering OFDM unfeasible due to its intrinsic drawbacks. Therefore, OFDM limitations such as the reduction in transmission throughput due to the use of cyclic prefix (CP), high peak-to-average power ratio (PAPR), sensitivity to carrier offset, and out-of-band emissions (OOB) are some of the problems solved in the proposed waveforms.

Attempts at combating some of the OFDM's limitations require an understanding of the root causes. For example, OOB emission (or spectral leakage) is introduced by band egress noise to neighboring bands and ingress noise from neighboring bands. This is because the spectral localization of the subcarriers is weak, resulting in spectral leakage. Filter bank multicarrier (FBMC) attempts to solve the aforementioned problem by direct suppression of the sidelobes using special filters. FBMC is spectrum-efficient, does not require redundant CP, and is robust to narrowband jammers. However, practical applications indicate that FBMC is vulnerable to multipath distortion due to a lack of CP. As a result, in practical cases whereby channel

state information is not perfect, OFDM will perform better. Attempt to improve FBMC and adopt it in MIMO channels has been reported in [10] with a focus on channel uncertainty.

There are other evident disadvantages of FBMC such as the introduction of overhead in overlapping symbols in the filter bank in the time domain and loss in bandwidth efficiency when transmitting short data packets. As a result, FBMC was extended to the generalized frequency division multiplex (GFDM) in [11]. GFDM is based on controlling the OOB of the transmitted signal by an adjustable pulse shaping filter applied to the individual carriers [12]. GFDM can be applied successfully in non-accurate synchronization of users without problems. However, the GFDM scheme is not perfect; adjacent synchronization is affected by some level of interference. Attempts at solving this problem have been exploited in [12, 13], but not without a significant increase in the transmitter's complexity.

Research progress led to circular FBMC (C-FBMC), a concept developed from GFDM and FBMC. C-FBMC is less complex, is easily extensible to the multiple-input multiple-output (MIMO) antenna, and preserves the orthogonality of the subcarrier's symbols. Most of the other proposed waveforms are based on the schemes described above. They either apply filtering or windowing operation (or both) in either the time or frequency domain. The aim of this section is not to review the literature but provide the basis for the waveform design. Therefore, to keep the content of this article concise, no further review will be pursued here. A detailed review is given in [14].

The discrete wavelet transform (DWT) is another potential waveform candidate for OFDM design. Its application in the OFDM is known as orthogonal wavelet division multiplex (OWDM). The DWT-based signal coding was introduced in [15] followed by many research studies. Some of them are documented in [16–22]. However, these research scopes are generally not broad enough to support the research insights into future wireless application requirements. OWDM's fit for 5G is scarcely reported in the literature. The contribution of this paper is addressing this by checking for both merits and demerits of using OWDM and weighing them against what the future wireless applications require. The 3rd Generation Partnership Project (3GPP) group has selected CP-OFDM (a holdover from 4G) as the signaling option for 5G for the 3GPP's Release 15. Therefore, we compared OWDM to CP-OFDM. We made a detailed comparison between Fourier transform-based CP-OFDM and OWDM using MATLAB, detailed its impact on healthcare, and proposed a guideline on how to approach wavelet application in 5G and beyond.

The rest of this paper is organized as follows: 5G design criteria and its impacts on healthcare are discussed in Section 2. Sections 3 and 4 are about the OFDM and OWDM system model. Section 5 contains simulations and results. Section 6 evaluates the results based on the requirements, while Section 7 draws conclusions and reviews based on the results.

2. 5G Design Criteria and Its Impacts on Healthcare

In order to give detailed simulation and comparison, we have taken into consideration all the necessary 5G KPIs [23] in gaging transmitter/receiver systems' efficiency.

2.1. High Energy Efficiency. In Section 1, we defined PAPR as the peak-to-average power ratio of the transmission and reception energy. Energy efficiency is mostly defined by the PAPR and degree of computational complexity. At the physical layer, waveforms exhibit peaks and lows. The implication is that, at transmission (or reception), if the difference (ratio) between the peaks and lows is large, higher transient energy will result in the power amplifiers which in turn will lead to higher energy consumption. Therefore, low PAPR is necessary for power-efficient transmissions at uplink (UL), downlink (DL), and side link (SL). Furthermore, computational complexity should be minimal, especially in power-stringent (battery-operated) devices such as the mobile phone or an IOT field sensor. In an IoT system, a further attempt at increasing the energy efficiency at the network layer has been reported in a recent study in [24]. It presents an information-centric networking (ICN) caching strategy that fits well in the energy-efficient IoT environment by utilizing Packet Update Caching (PUC). Considering all these advancements in research, it is safe to say the longevity of battery life and performance will be improved to ensure continuous and uninterrupted remote monitoring. Actually, in 5G, low-power sensors will be designed to operate on the same battery for the full duration of medical operation. This duration can be as much as 10 years [25].

2.2. Low Device Complexity. This section could also be termed as transceiver baseband complexity. It is the number of operations required to be performed to transmit and, more importantly, receive a signal successfully with the minimum possible processing overhead. At a very high frequency (e.g., millimeter-wave) and large bandwidths, severe RF impairments may result. With the presence of impairments, the waveform design standard should maintain the least possible computational complexity and processing overhead that could result from filtering, reduction of intersymbol interference (ISI) and intercarrier interference (ICI), windowing, interference cancellation, etc. The direct implication of this is battery longevity. This is similar to what is discussed above.

2.3. High Reliability. Reliability is evaluated by bit error rate (BER); it is the capability of a network to carry out a preferred operation with very low error rates. Biomedical sensors with IoT capabilities generate a huge amount of data, therefore error-sensitive. More so, considerable amounts of errors might lead to an increase in latency. Considering the signaling traffic from a massive number of these sensors would even lead to more increase in latency as each sensor is trying to retransmit. The low BER scheme will be supported by the 5G network. One of the main advantages of the proposed wavelet-OFDM scheme in this article is low BER compared to OFDM.

2.4. Low Latency. Ultralow latency defines the network which is optimized to process huge amounts of data packet with a very low tolerance for delay. 5G maximum allowed latency for the ultrareliable low-latency communication (URLLC) applications is less than 1 ms. This is due to services such as machine-to-machine communication requiring fast response time to allow efficient sporadic transmission of small packets. So, it requires a transmission mode with low air-interface latency enabled by very short frames. The efficient transmission of short frames is very much essential for medical IoT. For example, in telesurgery, the maximum acceptable latency (end-to-end) is 200 ms [26]. Comparing this to the 5G network typical latency of less than 1 ms, "telesurgeons" can be guaranteed low latency communication and optimum stability in receiving haptic feedback and improved wireless data rates for better visualization and greater precision. In the future, this will serve as an enabling technology for new telesurgery applications alongside other real-time applications with stricter latency requirements. This can also serve as an enabling technology for emerging e-health fields requiring some forms of wireless transfer of big data and machine learning for early detection of certain diseases. These diseases are not limited to heart disease [27], Parkinson [28], and breast cancer [29]. For further studies about latency reduction in 5G, refer to [30].

2.5. High Spectral Efficiency or High Bandwidth. Bandwidth refers to the transmission capacity of a network per given time. Spectral efficiency refers to the efficient use of the available bandwidth. In the 3G and 4G networks, biomedical sensors can only send a limited amount of data due to restricted bandwidth [31]. This limitation is mitigated in 5G by exploring the available (untapped) spectrum at higher frequencies (as high as 10 GHz). Also, at such high frequencies, a higher transmission rate on the order of Gbps is achieved. With this, seamless remote monitoring can be achieved; physicians can view ultra-high-definition contents (videos and pictures) and be able to make better-informed decisions. Furthermore, online consultations can be carried out whereby patients, ordinary citizens, different civic associations, experts, and executive bodies can contribute and exchange medical information.

Having discussed the benefits of 5G's high spectral efficiency, it is necessary to note that several factors could also contribute to the degradation of its spectral efficiency (Sections 5.3 and 5.4). This is why the nature of the waveform is more important. This is one of the problems addressed in the waveform scheme proposed in this article.

2.6. Massive Asynchronous Transmission. Massive asynchronous transmission or asynchronous coexistence of a huge number of nodes will be achieved with 5G. This will be achieved with D2D [32]. In D2D communications, each

terminal can communicate with each other directly without routing through gateways and base stations. Therefore, a highly dense network problem can be solved through D2D communications. D2D communications will enable asynchronous coexistence between a large number of medical sensors, wearables, and devices, and monitoring equipment can communicate with minimal interference.

In the 4G network, all communications are routed through gateways and base stations. This routing is inefficient, especially when devices are near each other. Achieving D2D communication will require waveforms with less strict synchronization requirements [33]. The effect of poor synchronization is phase noise. Phase noise including carrier frequency offset (CFO) is both caused by differences in the transmitter and receiver oscillator. The mathematical description of the CFO is the multiplication of a signal in the time domain by a time-varying complex exponential function. CFO will cause a received signal to be shifted in the frequency. Therefore, sampling of the received signal will be done at an offset point, which is not the peak point. The result is a raised ICI [8].

2.7. MIMO Compatibility. Massive MIMO is a key technology in delivering mobile 5G. This is essentially grouping together large-scale antennas at the transmitter and receiver to increase throughput and improve spectrum efficiency at the access nodes. Other benefits of massive MIMO are lower latency, simplification of the media access control (MAC) layer, and robustness against (intentional) jamming. Furthermore, beamforming is necessary for overcoming high propagation losses especially at very high frequencies. One of the direct impacts and implications of this is large file transfers. Hospitals will possess the ability to transfer large image files such as medical images. Overall, hospitals will be able to process more patients, given the same amount of time.

One of the various checks of our proposed waveform is its suitability and ease of integrating MIMO with it. It should be less complex and practicable.

2.8. Robustness to Frequency-Selective and Time-Selective Channels. Very harsh propagation conditions can cause poor performance in a wireless communication system and result in a loss of signal power without loss of noise power, consequently resulting in a poor signal-to-noise ratio (SNR). OFDM is generally used to combat selective fading because of its robustness to frequency-selective channels. Among other methods are MIMO, rake receivers, space-time codes, forward error correction, interleaving, etc. The robustness of the 5G waveform design should include adapting to this impairment as well as time-selective fading occurring in high-speed scenarios. An example of such a case is the vehicle to anything (V2X). In this case, we can consider the (efficient) transmission of the medical ultrasound video stream from a fast-moving ambulance to the host hospital.

3. OFDM System Model

OFDM is the most popular multicarrier modulation scheme that is currently being employed in many standards such as the downlink of 4G LTE and the IEEE 802.11 family [34]. In an OFDM system, at the transmitter, data to be transmitted are mapped to a constellation, split into parallel, and modulated using the inverse fast Fourier transform (IFFT). The modulation process is shown in Figure 1. Guard band and cyclic prefix (CP) are inserted to prevent a delayed version of symbol overlapping with the adjacent symbol and mitigate the delay spread, respectively. The orthogonal signals are then mixed. The key process here is modulation, where signals are mapped from the frequency domain to the time domain and multiplexed. The modulation process is mathematically the summation of N tones described in [35] and mathematically expressed in the following equation:

$$x_n(t) = \sum_{k=0}^{N-1} s_k[n]e^{j((2k\pi)/T)t}. \tag{1}$$

$x_n[t]$ is the summation of the number of complex-valued sinusoids N with period T in the continuous-time domain t. n denotes the discrete-time index. The data symbol is $s_k[n]$, with frequency component $k = 0, 1, \ldots, N-1$. The multiplexed data symbol $y_n(t)$ on the baseband is passed through a channel with transfer function $H(f)$, which is expressed mathematically in the following equation:

$$y_n(t) = \sum_{k=0}^{N-1} H\left(\frac{k}{t}\right) s_k[n]e^{j(2k\pi/T)t}. \tag{2}$$

The sinusoids N are located at frequencies $f = 0, 1/T, 2/T, \ldots, (N-1)/T$ for orthogonality. The orthogonality between two adjacent sinusoids is defined in the following equation:

$$\sum_{t=N/2}^{N/2} e^{-j2\pi kt/N} e^{-j2\pi pt/N} = 0, \quad \forall p \neq k. \tag{3}$$

After modulation, the CP denoted as p is added by copying the last part of the modulated IFFT signal and appending it to the beginning as a guard interval to prevent ISI. In the 4G LTE system, the CP is hard-coded into the waveform, while for 5G NR Release 15, the CP is determined by the maximum delay present in individual channels.

At the receiver, the transmitting process is reversed to decode the received data. For demodulation, the fast Fourier transform (FFT) is employed. OFDM, as opposed to a single-carrier system, has the ability to cope with frequency-selective fading because data are divided and transmitted in parallel streams on a modulated set of subcarriers. This approach results in the efficient use of bandwidth.

4. OWDM System Model

Some of the wavelet transform applications are in source and channel coding, signal denoising, and data compression [36, 37]. DWT and inverse discrete wavelet transform (IDWT) are used in OWDM [38, 39]. This replacement is
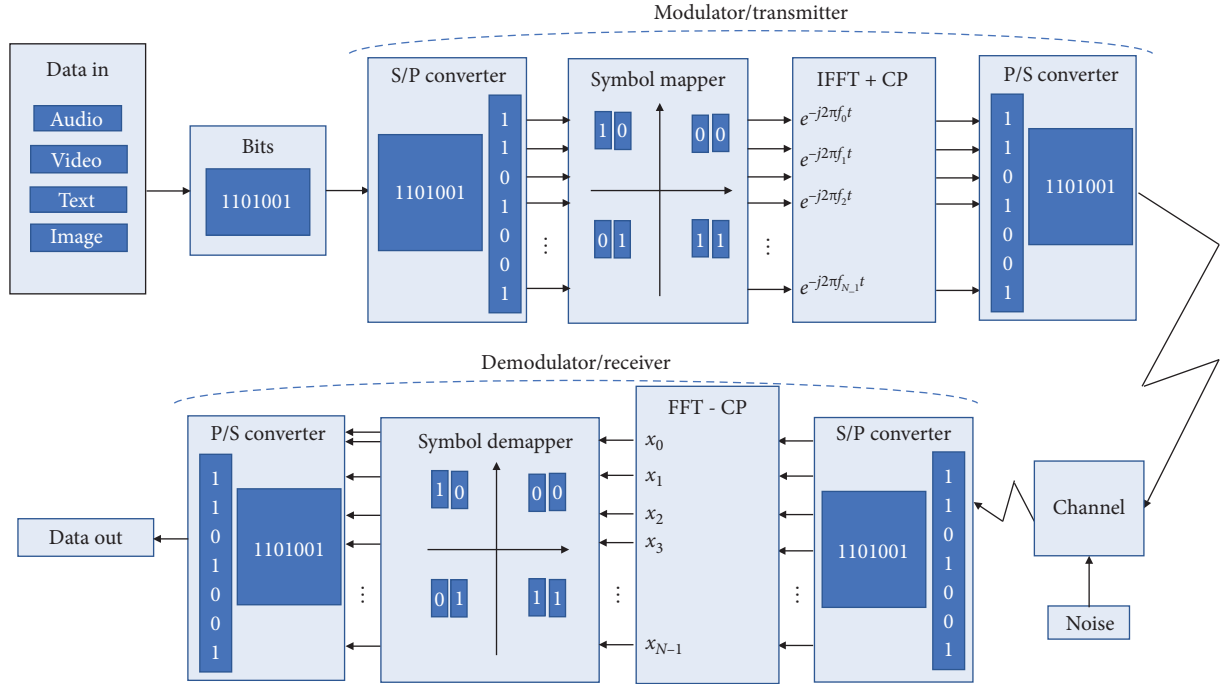
FIGURE 1: Fourier-OFDM modulation and demodulation system process model.

due to its properties such as orthonormality [40–42] and the ability to decompose signals effectively in the time-frequency domains by scaling and shifting. In DWT, the scaling (j) and shifting (k) results are generated by the mother wavelet denoted by Ψ as a function of time (t) and mathematically expressed in the following equation:

$$\Psi_{J,K}(t) = 2^{-j/2}\Psi(2^{-j}t - k). \tag{4}$$

The discrete wavelet and the inverse discrete wavelet representation of a signal are given by equations (5) and (6), respectively [43]:

$$X_{\mathrm{DWT}k}^{j} = \int_{-\infty}^{\infty} x(t)^{j/2}\Psi(2^{j}\ t - k)\mathrm{d}t, \tag{5}$$

$$X_{\mathrm{IDWT}}(t) = \sum_{j=-\infty}^{\infty} \cdot \sum_{k=-\infty}^{\infty} X_{k}^{j} 2^{j/2}\Psi(2^{j}\ t - k)\mathrm{d}t. \tag{6}$$

x is the input signal in the time domain. Therefore, the OWDM symbol can be expressed as the weighted sum of wavelet and scale carriers and is mathematically expressed in the following equation:

$$S(t) = \sum_{j \leq J} \cdot \sum_{k} w_{j,k}(t).\Psi_{j,k}(t) + \sum_{k} a_{j,k}.\varnothing_{J,k}(t). \tag{7}$$

$w_{j,k}$ is the sequence of the wavelet, and $a_{J,k}$ are the approximation coefficients.

The OWDM transmission and reception concept is the same with the OFDM; however, the modulation process is different. It makes use of IDWT for modulation and DWT for demodulation. This is highlighted in Figure 2. Starting with the modulation process, the data bits are mapped into OFDM symbols of parallel data stream corresponding to the number of subcarriers. This signal is converted to serial $X(n)$ and fed into IDWT. Here, the signal is vector-transposed (V_t), upsampled (u_s), and convoluted with a low-pass filter (LPF) and high-pass filter (HPF) [44] using approximated coefficients (A_c) and detailed coefficients (D_c), respectively. The decomposed outputs from the LPF and HPF are $L(n)$ and $H(n)$, respectively. Different wavelet families have different filter lengths, so the length of the zero pads is adjusted accordingly to maintain orthonormality and orthogonality in $L(n)$ and $H(n)$. $L(n)$ and $H(n)$ are mixed and then transmitted.

At the receiver, the modulation process is simply reversed to decode the received data. The received data are decomposed back into $L(n)$ and $H(n)$ using the LPF and HPF, respectively. $H(n)$ contains noise, so it is discarded, while $L(n)$ is processed for data recovery. In this paper, for our analysis, we considered Haar, Daubechies (DB2), biorthogonal (Bior5.5), and Symlet (Sym4) wavelet transforms. Our consideration is based on the results in [45–47]. The results show that these transforms are the most suitable for waveform design because of their resiliency to channel noise.

4.1. Haar Wavelet.
The Haar wavelet, discovered by a Hungarian mathematician [48], is a sequence of rescaled "square-shaped" functions which together form a wavelet family or basis. Both wavelet function and scaling function are square-shaped as shown in Figures 3 and 4. The simplest example of an orthogonal wavelet is the Haar function
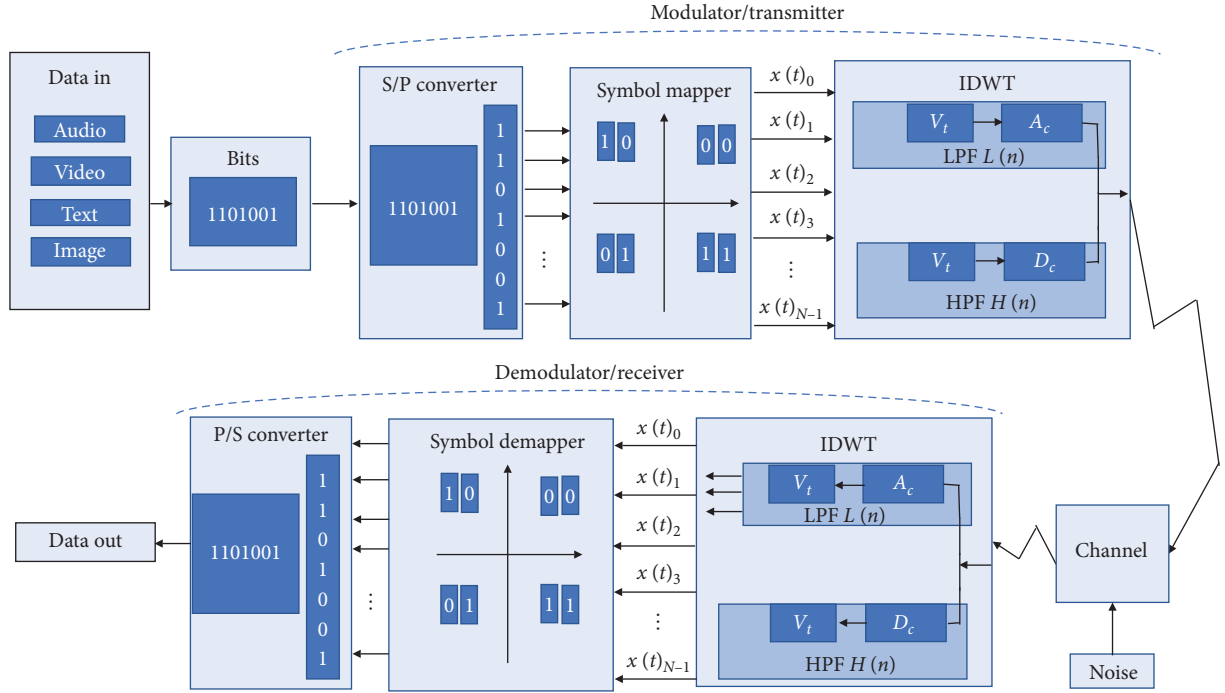
Modulator/transmitter

Figure 2: Wavelet-OWDM modulation and demodulation system process model.
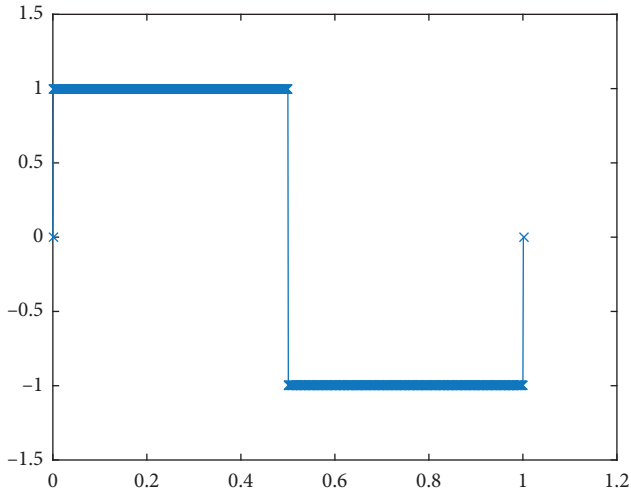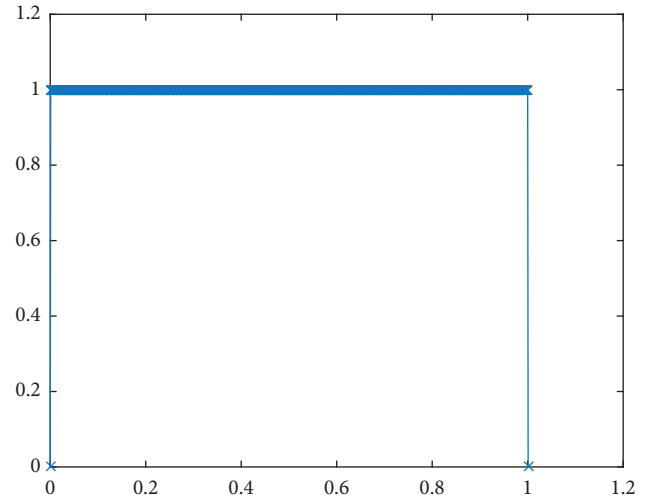

Figure 3: Haar wavelet function.

Figure 4: Approximation of the Haar scaling function.

denoted by ΨH and defined by [49] and mathematically expressed in equations (8) and (9):

$$\Psi(t) = \begin{cases} 1, & \text{for } 0 \le x < \dfrac{1}{2}, \\ -1, & \text{for } \dfrac{1}{2} \le x < 1, \\ 0, & \text{otherwise.} \end{cases} \qquad (8)$$

Its scaling function $\varphi(t)$ can be described as

$$\Phi(t) = \begin{cases} 1, & 0 \le t < 1, \\ 0, & \text{otherwise.} \end{cases} \qquad (9)$$

4.2. Daubechies Wavelet.
Daubechies wavelet is orthogonal, and it is characterized by a maximal number of vanishing moments for some given support. Daubechies wavelets are usually characterized by *dbN*, *N* referring to the order number. Figures 5 and 6 demonstrate the Db4 wavelet and scaling functions. In this paper, the Db4 wavelet is used.

4.3. Symlet Wavelet.
The Symlet wavelet transforms are in the *N* order (Sym4); in this paper, we used the Sym4 wavelet. The Symlets are orthogonal, nearly symmetrical, and biorthogonal wavelets. They are a modification of the Db family to improve symmetry [50]. Figures 7 and 8 represent the Sym4 wavelet and scaling functions.
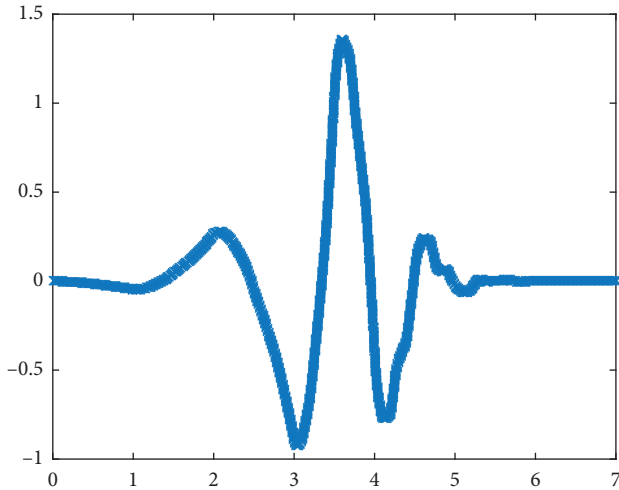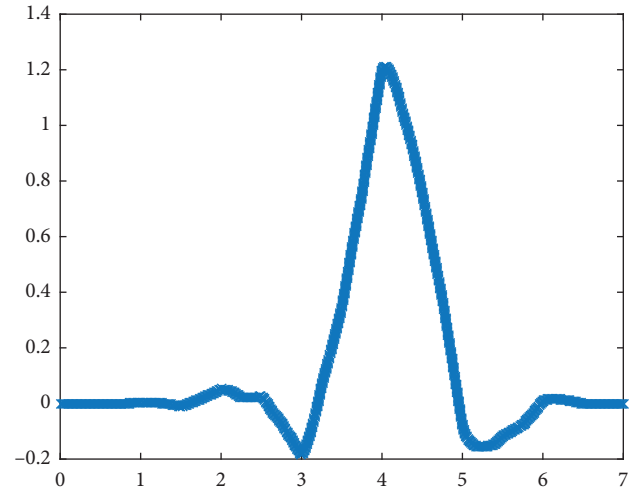
FIGURE 5: Approximation of the Db4 wavelet function.
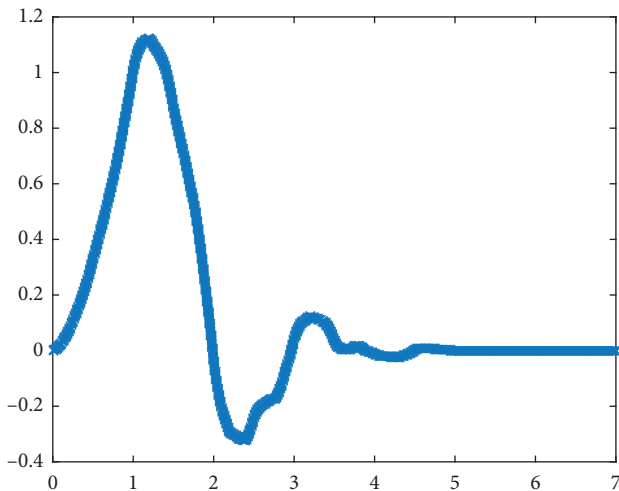

FIGURE 6: Approximation of the Db4 scaling function.

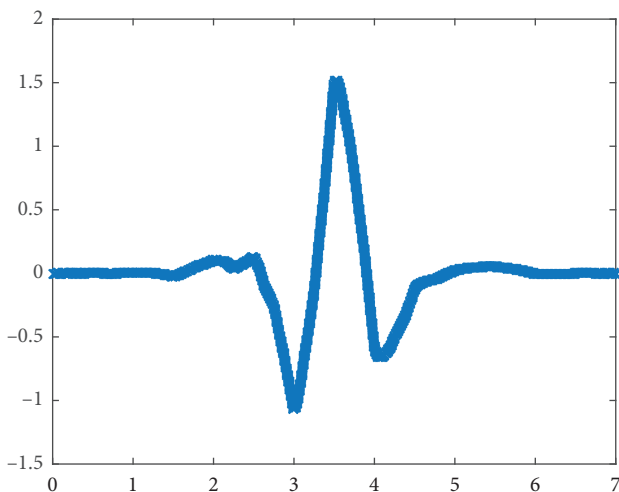FIGURE 7: Approximation of the Sym4 wavelet function.

FIGURE 8: Approximation of the Sym4 scaling function.

4.4. Biorthogonal Wavelet. This is a wavelet function where the associated wavelet transform is invertible but not necessarily orthogonal. In many cases, it is required to choose a wavelet and scaling function such that they meet the condition of mirrored impulse response filters, without the loss of orthogonality [51]. In the biorthogonal case, there are two scaling functions for decomposition and reconstruction which must satisfy the following biorthogonality condition and are expressed mathematically in equation (10) and graphically demonstrated in Figures 9 and 10.

$$\sum_{n\varepsilon\mathbb{Z}}^{\infty} a_n \tilde{a}_{n+2m} = 2.\delta_{m,0}. \tag{10}$$

5. Simulation Results' Analysis

Here, a grayscale image having resolution 800×800 pixels of 8 bits depth is fed into the MATLAB simulator as the test data. In total, the image has 5,120,000 bits, which are enough for our simulation. The simulation parameters for the OFDM and OWDM are shown together in Table 1. The major impacting factor is the communication channel. For a more practical approach, we considered the additive white Gaussian noise (AWGN) channel.

5.1. BER Performance Analysis. Here, we present the BER versus SNR plot for each candidate and also some images to show their qualities at a varied SNR. An AWGN channel is assumed. From the graphical result, the wavelet transforms show a lower BER than the Fourier transforms and wider BER performance with increasing SNR in Figure 11. The lower BER result is due to the wavelet-based waveform having properties such as orthonormality and the ability to encode signals both with time and frequency localization simultaneously as opposed to Fourier transform which can
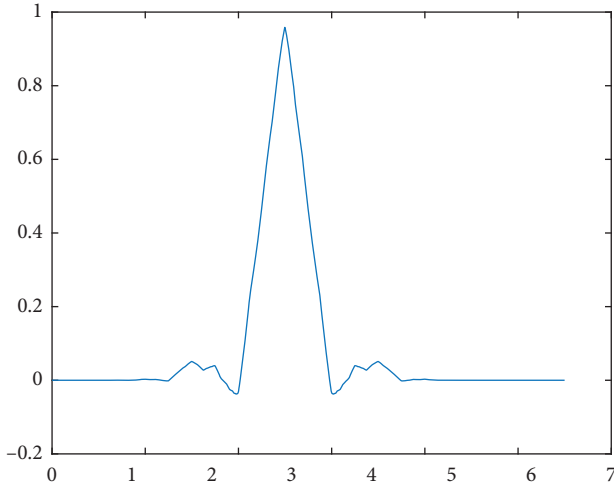
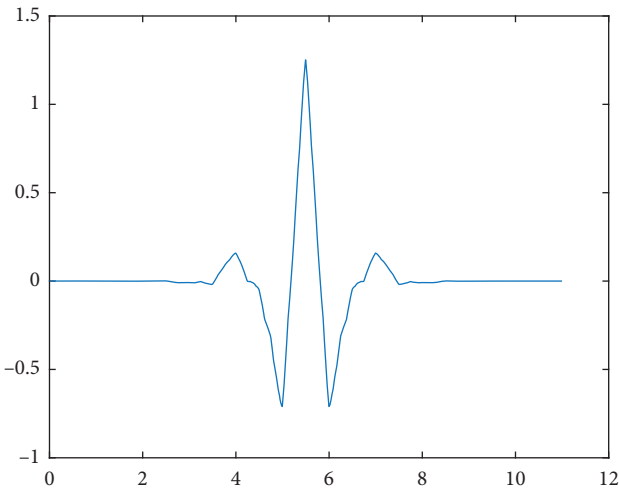FIGURE 9: Approximation of the biorthogonal wavelet function.

FIGURE 10: Approximation of the biorthogonal scaling function.

TABLE 1: Simulation parameters for OFDM and OWDM.

Modulation	QPSK
FFT size	1024
Number of subcarriers	128
CP length	16
SNR range	1 db–10 db
Channel	AWGN, Rayleigh
Maximum Doppler frequency	0 Hz
Sampling period	$1e3$
Path delays	$0, 1e-3, 3.5e-5, 12e-5$
Path gains	$0, -1, -1, -3$
Carrier frequency	7 GHz
CFO	100 Hz
Wavelet transforms	Biorthogonal 5.5 Haar Symlet4 Daubechies4

only analyze signals with time localization only. This wavelet transform property enables efficient encoding (and decoding) of signals, hence the robustness to the channel error.
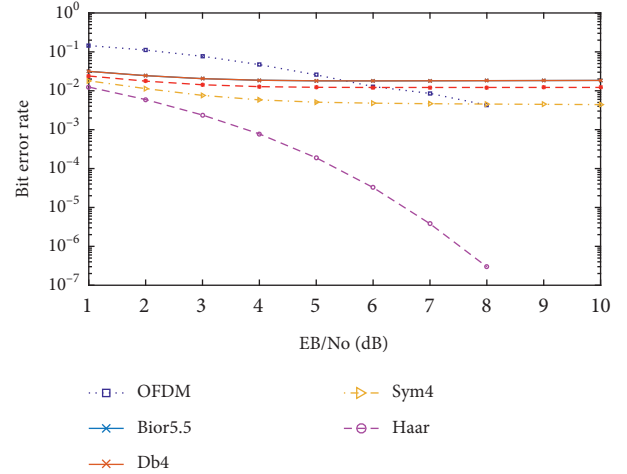

FIGURE 11: BER performance comparison in the AWGN channel.

5.2. PSD and PAPR Performance. The PAPR is a KPI of a wireless communication system as it goes a long way in shaping the design of the power amplifier's level of linearity and therefore its cost. PAPR is evaluated by computing the complementary cumulative distribution function (CCDF) of the waveform with respect to the number of subcarriers and constellation order. Transmit PAPR performance is given in Table 2, and the plot of the received PAPR against a varied SNR is shown in Figure 12 for the Fourier-OFDM and the wavelet modulations.

At transmission and at reception with a varied SNR of 1 dB to 10 dB, all the wavelet variants have better and distinct PAPR performance than the OFDM with the Haar wavelet having the best performance. Although the wavelet transforms have lower PAPR, they use more transmit power than Fourier. In Figure 12, a plot of the received PAPR at various SNRs is shown, including the power spectral density performance (PSD images) of various transforms at 128 subcarriers each.

In a nonlinear amplifier, OFDM is susceptible to spectral regrowth compared to other wavelets due to its high PAPR. The theory behind this is the broadening of a bandwidth of a modulated signal with large envelope fluctuations due to nonlinearities that generate mixing products between the individual frequency components of the spectrum. The end result is adjacent channel interference. Figures 13–17 are the PSD plots of various transforms. OFDM has a higher sidelobe (noise) than the rest of the wavelet transforms.

Table 3 is the bandwidth result from transmitting the test data at 7 GHz as specified at the beginning of this section. The very high use of bandwidth by Fourier (low spectral efficiency) is as a result of the need for cyclic prefixing.

5.3. Effect of the Carrier Frequency Offset. In this section, we assume that both users are perfectly synchronized in the time domain but with an offset between their respective carrier frequencies. In Figure 18, we present the BER curve at CFO = 0.1 kHz. The simulation result shows that OFDM suffers the most effect from CFO, while Haar incurs the least effect. Also, it is observed that the performance disparity between the transforms increases roughly with the SNR.

TABLE 2: Transmit PAPR of various transforms and the transmit power.

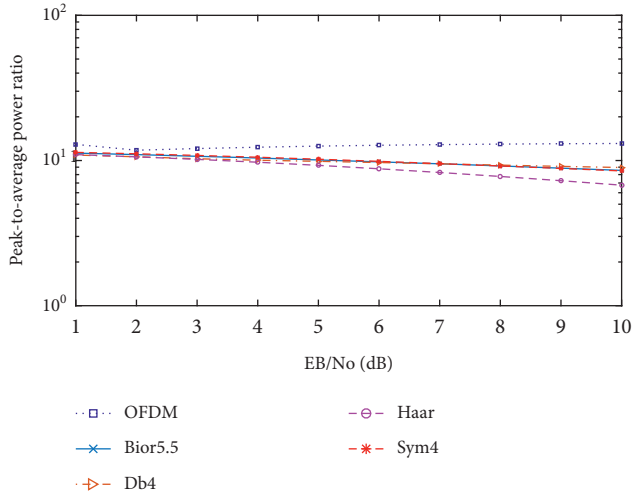| Transform	Transmit PAPR (dB)	Transmit power (dB)
Fourier	18.95	−21.10
Haar	$1.93e − 15$	−6.04
Sym4	5.35	−6.04
Db4	7.18	−6.04
Bior5.5	6.87	−3.67

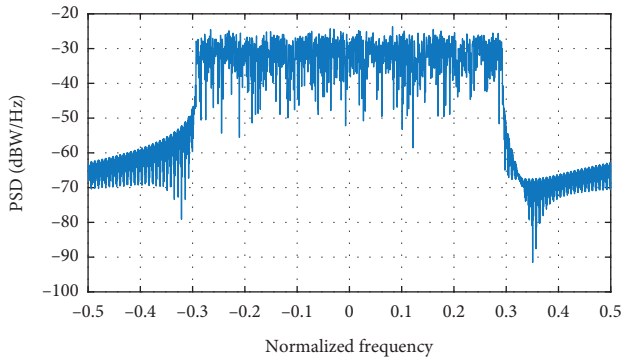FIGURE 12: Received PAPR performance of various transforms.
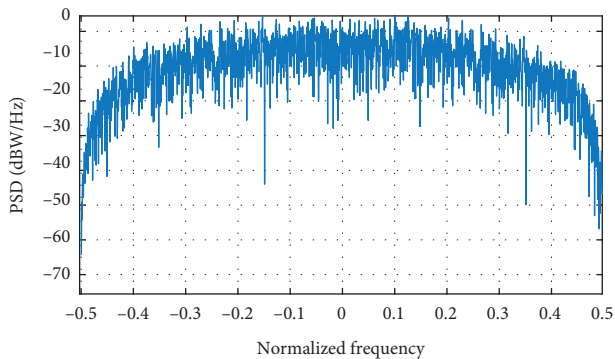

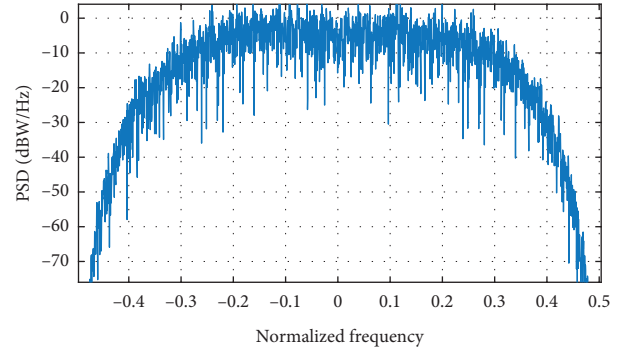FIGURE 13: OFDM PSD plot.

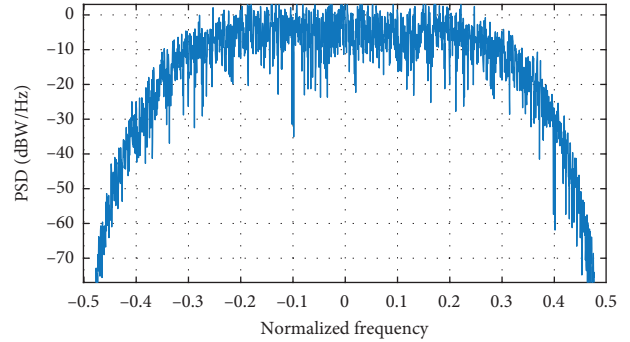FIGURE 14: Haar PSD plot.

FIGURE 15: Sym4 PSD plot.

FIGURE 16: Db4 PSD plot.
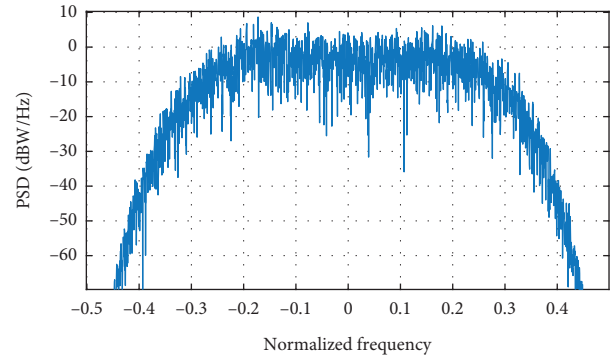
FIGURE 17: Bior5.5 PSD plot.

TABLE 3: Occupied bandwidth of various transforms at 7 GHz.

Transform	Bandwidth (Hz)
Fourier	418.615
Bior5.5	286.212
Haar	363.605
Sym4	376.248
Db4	374.307

5.4. Effect of Multipath Fading. The test data as described at the beginning of Section 5 are transmitted and received using various transforms to measure the impact of multipath fading on them. The simulation parameters are also exactly as given in the aforementioned section, i.e., four taps with their respective channel gains in a Rayleigh multipath fading channel. In order to observe the maximum BER per SNR, channel state

FIGURE 18: BER versus Eb/No at CFO = 0.1 kHz.
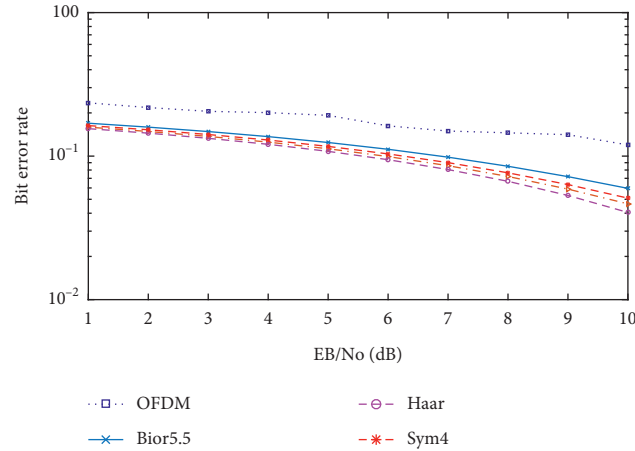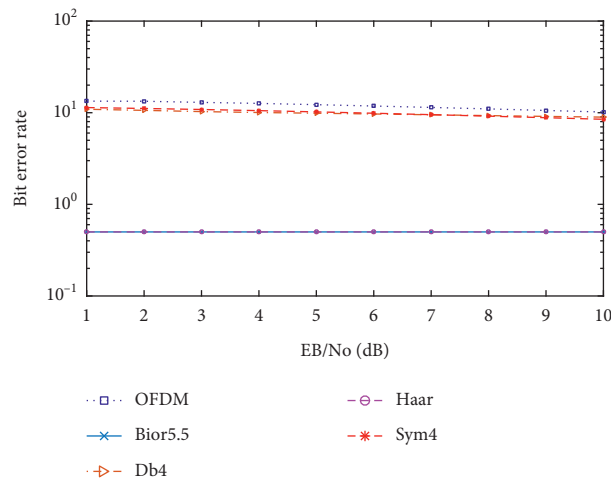

FIGURE 19: OFDM and OWDM BER vs. SNR in the frequency-selective Rayleigh fading channel.

TABLE 4: Overhead of various transforms.

Transform	Time (ms) Modulation + demodulation	Peak Mem (MB) Modulation + demodulation
Fourier	212	90
Haar	1980	320
Bior5.5	2215	308
Sym4	2209	312
Db4	2239	312

information (CSI) and equalization were not considered. It is observed that the OWDM transforms are considerably robust to the multipath fading effect. In Figure 19, OFDM and OWDM's BER vs. SNR in the frequency-selective Rayleigh fading channel are graphically demonstrated.

5.5. Overhead Cost and Complexity of Implementation. The time and memory requirements for both at the transmitter and at the receiver are simulated and shown in Table 4. The simulation of the overhead cost is based on the transmission and reception of the image with the size as described at the beginning of Section 4. For the purpose of accuracy, the time and memory computation costs are limited to IFFT/FFT and IDWT/DWT only.

In Table 4, it is observed that although OWDMs might seem like an attractive choice, they generally require more computational resources than the OFDM.

6. OFDM and OWDM Evaluation Metrics

Using the simulation results above, we assess OFDM and OWDM for a number of KPIs, taking the 5G set standards into consideration. These comparisons are outlined in Table 5.

TABLE 5: Comparative analysis of OFDM and OWDM.

5G performance metrics	Fourier	Haar	Db2 Sym4 Bior5.5
High energy efficiency	PAPR is high. Computational complexity is low.	PAPR is low, and computational complexity is high. Haar has the lowest processing time, but memory requirement is higher than other wavelet pairs.	
Low device complexity	Needs one block per process; IFFT and FFT.	Require a larger device processing capacity. Wavelet transforms generally need two blocks (i.e., their filter banks) for each process (i.e., IDWT and DWT) and more memory than Fourier. However, advances in the clock speeds and memory sizes of communication devices have increased by 4 to 6 orders of magnitude in the past 40 years [52]. Therefore, future wise, complexity might not be a challenge.	
High reliability	Has poorer BER performance compared to OWDM.	Have better BER performance under a wide varied SNR.	
Low latency	Requires the use of CP to reduce ISI which resultantly reduces throughput.	Do not require CP.	
High spectral efficiency	It has a considerable spectral efficiency.	They have better spectral efficiency compared to Fourier due to Fourier's requirement of higher bandwidth (CP).	
Massive asynchronous transmission	Spectral localization of the subcarriers is weak and highly susceptible to the CFO effect.	They are more localized in time and space. Consequently, they are more immune to the CFO effect.	
MIMO compatibility	OFDM is quite compatible with MIMO because of its ease of implementation.	The use of OWDM with MIMO is feasible and has been documented in the literature [36].	
Frequency-time channel selectivity	OFDM is robust to frequency-selective channels and can be made robust to time channel selectivity by a proper choice of subcarrier spacing.	OWDM is more robust to frequency-selective channels, especially at low SNRs.	
Flexibility and scalability	By proper choice of design parameters, OFDM is a flexible waveform that can support diverse services, with several evolved versions.	OWDM is also a flexible waveform. More so, there are different wavelet transforms with different scalable properties. Therefore, its flexibility [53] could be explored and tailored to the requirements of the 5G NR classifications.	

TABLE 6: Proposed assessment of OFDM and OWDM for 5G NR.

Performance indicators	OFDM assessment	OWDM assessment	Downlink requirement	Uplink requirement	Side link requirement	V2X requirement	Backhaul requirement
Spectral efficiency	High	Very high	Very high	Very high	High	Very high	Very high
MIMO compatibility	High	High	Very high	Very high	High	Very high	Very high
Time localization	High	Very high	High	High	High	Very high	Very high
Transceiver baseband complexity	Low	High	Very high	High	Very high	High	High
Robustness to frequency-selective channels	High	High	High	High	High	High	High
Robustness to time-selective channels	Medium	High	High	High	High	Very high	Low
Robustness to phase noise	Medium	High	High	High	High	High	High
Robustness to sync errors	High	Very high	Low	High	High	Medium	Low
PAPR	High (can be reduced)	Low	Low	High	High	Medium	Low
Frequency localization	Low (can be reduced)	High	Medium	Medium	Medium	Medium	Low

The proposed application guidelines are given in Table 6 based on the 5G NR design criteria and waveform assessment discussed in [54].

7. Conclusion

The research presented in this paper provides a deep insight into the consideration of OWDM for 5G NR physical layer design and beyond. KPI assessment of OFDM and OWDM and their respective performance simulation results have been carried out. Our results show that OWDM outperforms OFDM in many of the KPIs, and it is, therefore, a more efficient IoT enabler for healthcare and other vital areas. However, our results also show that the main drawback of OWDM is high memory and time cost. In view of this, careful tradeoff considerations are required. Furthermore, we also include uplink, downlink, side link, V2X, and backhaul links as further assessments. These various link assessments are necessary for OWDM waveform numerology establishments for 5G's diverse applications. Finally, we observed that, in the establishment of OWDM waveform numerologies for 5G, CP will not be required. This means the establishment process can be less complicated than that of OFDM.

Data Availability

No data were used to support this study.

Conflicts of Interest

The authors declare that there are no conflicts of interest regarding the publication of this paper.

Acknowledgments

References

[1] A. Ijaz, L. Zhang, M. Grau et al., "Enabling Massive IoT in 5G and beyond systems: PHY radio frame design considerations," *IEEE Access*, vol. 4, pp. 3322–3339, 2016.

[2] S. B. Baker, W. Xiang, and I. Atkinson, "Internet of things for smart healthcare: technologies, challenges, and opportunities," *IEEE Access*, vol. 5, pp. 26521–26544, 2017.

[3] S. K. Goudos, M. Deruyck, D. Plets et al., "A novel design approach for 5G massive MIMO and NB-IOT green networks using a hybrid Jaya-differential evolution algorithm," *IEEE Access*, vol. 7, pp. 105687–105700, 2019.

[4] T. S. Rappaport, Y. Xing, O. Kanhere et al., "Wireless communications and applications above 100 GHz: opportunities and challenges for 6G and beyond," *IEEE Access*, vol. 7, pp. 78729–78757, 2019.

[5] A. B. Kihero, M. S. J. Solaija, and H. Arslan, "Inter-numerology interference for beyond 5G," *IEEE Access*, vol. 7, pp. 146512–146523, 2019.

[6] Y. Medjahdi, S. Traverso, R. Gerzaguet et al., "On the road to 5G: comparative study of physical layer in MTC context," *IEEE Access*, vol. 5, pp. 26556–26581, 2017.

[7] C. An and H. Ryu, "CPW-OFDM (cyclic postfix windowing OFDM) for the B5G (Beyond 5th Generation) waveform," in *Proceedings of the IEEE 10th Latin-American Conference on Communications (LATINCOM)*, pp. 1–4, Guadalajara, Mexico, November 2018.

[8] F. Kalbat, A. Al-Dweik, B. Sharif, and G. K. Karagiannidis, "Performance analysis of precoded wireless OFDM with carrier frequency offset," *IEEE Systems Journal*, vol. 14, 2020.

[9] O. Daoud, "Power reallocation and complexity enhancement for beyond 4G systems," *China Communications*, vol. 16, no. 6, pp. 114–128, 2019.

[10] M. Payaró, A. Pascual-Iserte, and M. Najar, "Performance comparison between FBMC and OFDM in MIMO systems under channel uncertainty," in *Proceedings of the European Wireless Conference (EW)*, pp. 1023–1030, Lucca, Italy, April 2010.

[11] G. Fettweis, M. Krondorf, and S. Bittner, "GFDM-generalized frequency division multiplexing," in *Proceedings of the IEEE 69th Vehicular Technology Conference (VTC)*, pp. 1–4, Barcelona, Spain, April 2009.

[12] N. Michailow, I. Gaspar, S. Krone, M. Lentmaier, and G. Fettweis, "Generalized frequency division multiplexing: analysis of an alternative multi-carrier technique for next generation cellular systems," in *Proceedings of the 2012 International Symposium on Wireless Communication Systems (ISWCS)*, pp. 171–175, Paris, France, August 2012.

[13] M. Matthe, L. L. Mendes, and G. Fettweis, "Space-time coding for generalized frequency division multiplexing," in *Proceedings of the 20th European Wireless Conference*, pp. 1–5, Barcelona, Spain, May 2014.

[14] B. Farhang-Boroujeny and H. Moradi, "OFDM inspired waveforms for 5G," *IEEE Communications Surveys & Tutorials*, vol. 18, no. 4, pp. 2474–2492, 2016.

[15] M. A. Tzannes and M. C. Tzannes, "Bit-by-bit channel coding using wavelets," in *Proceedings of the [Conference Record] GLOBECOM'92-Communications for Global Users*, vol. 2, pp. 684–688, Orlando, FL, USA, December 1992.

[16] M. Chafii, Y. J. Harbi, and A. G. Burr, "Wavelet-OFDM vs. OFDM: performance comparison," in *Proceedings of the 23rd International Conference on Telecommunications (ICT)*, pp. 1–5, Thessaloniki, Greece, May 2016.

[17] S. A. Dawood, F. Malek, M. S. Anuar, and S. Q. Hadi, "Discrete multiwavelet critical-sampling transform-based OFDM system over Rayleigh fading channels," *Mathematical Problems in Engineering*, vol. 2015, Article ID 676217, 10 pages, 2015.

[18] K. Lavish, V. Sharma, and J. S. Malhotra, "MIMO-WiMAX system incorporated with diverse transformation for 5G applications," *Frontiers of Optoelectronics*, vol. 12, pp. 1–15, 2019.

[19] R. Ayeswarya and N. Amutha Prabha, "Fractional wavelet transform based OFDM system with cancellation of ICI," *Journal of Ambient Intelligent Humanized Computing*, 2019.

[20] S. Tripathi, A. Rastogi, K. Sachdeva, M. K. Sharma, and P. Sharma, "PAPR reduction in OFDM system using DWT with nonlinear high-power amplifier," *International Journal of Innovative Technology and Exploring Engineering (IJITEE)*, vol. 2, no. 5, pp. 2278–3075, 2013.

[21] N. Ali, M. I. Youssef, and I. F. Tarrad, "ICI reduction by parallel concatenated encoder using wavelet transforms," *Advances in Intelligent Systems and Computing*, vol. 933, 2020.

[22] J. Lee and H. Ryu, "Design and comparison of discrete wavelet transform based OFDM (DWT-OFDM) system," in *Proceedings of the Tenth International Conference on Ubiquitous and Future Networks (ICUFN)*, pp. 881–885, Prague, Czech Republic, July 2018.

[23] A. F. Demir, M. Elkourdi, M. Ibrahim, and H. Arslan, "Waveform design for 5G and beyond," *5G Networks: Fundamental Requirements, Enabling Technologies, and Operations Management*, pp. 51–76, 2018.

[24] I. U. Din, S. Hassan, A. Almogren, F. Ayub, and M. Guizani, "PUC: packet update caching for energy efficient IoT-based information-centric networking," *Future Generation Computer Systems*, vol. 111, pp. 634–643, 2020.

[25] H. T. Mouftah, M. Erol-Kantarci, and M. H. Rehmani, *Transportation and Power Grid in Smart Cities: Communication Networks and Services*, Wiley, Hoboken, NJ, USA, 2018.

[26] Q. Han, S. Liang, and H. Zhang, "Mobile cloud sensing big data and 5G networks make an intelligent and smart world," *IEEE Networks*, vol. 29, no. 2, pp. 40–45, 2015.

[27] U. H. Amin, J. P. Li, M. H. Memon, S. Nazir, and R. Sun, "A hybrid intelligent system framework for the prediction of heart disease using machine learning algorithms," *Mobile Information Systems*, vol. 2018, Article ID 3860146, 21 pages, 2018.

[28] A. U. Haq, J. P. Li, M. H. Memon et al., "Feature selection based on L1-norm support vector machine and effective recognition system for Parkinson's disease using voice recordings," *IEEE Access*, vol. 7, pp. 37718–37734, 2019.

[29] U. H. Amin, "A novel integrated diagnosis method for breast cancer detection," *Journal of Intelligent and Fuzzy Systems*, vol. 38, pp. 1–16, 2020.

[30] M. Simsek, A. Aijaz, M. Dohler, J. Sachs, and G. Fettweis, "5G-enabled tactile Internet," *IEEE Journal on Selected Areas in Communications*, vol. 34, no. 3, pp. 460–473, 2016.

[31] O. O. Fagbohun, "Comparative studies on 3G,4G and 5G wireless technology," *IOSR Journal of Electronics and Communication Engineering*, vol. 9, no. 2, pp. 133–139, 2014.

[32] V. Kumar, S. Yadav, D. N. Sandeep, S. Dhok, R. K. Barik, and H. Dubey, "5G cellular: concept research work and enabling technologies," in *Advances in Data and Information Sciences*, pp. 327–338, Springer, Singapore, 2019.

[33] A. Ahad, M. Tahir, and K. A. Yau, "5G-Based smart healthcare network: architecture, taxonomy, challenges and future research directions," *IEEE Access*, vol. 7, pp. 100747–100762, 2019.

[34] T. Hwang, C. Yang, G. Wu, S. Li, and G. Ye Li, "OFDM and its wireless applications: a survey," *IEEE Transactions on Vehicular Technology*, vol. 58, no. 4, pp. 1673–1694, 2009.

[35] M. Veena and S. Shanmukha, "Performance analysis of DWT based OFDM over FFT based OFDM and implementing on FPGA," *International Journal of VLSI Design & Communication Systems*, vol. 2, pp. 119–130, 2011.

[36] G. K. Rao and A. S. S. Rao, "Performance analysis of adaptive MIMO based OFDM using FFT and DWT," *International Journal of Advanced Research in Science and Technology*, vol. 4, pp. 262–266, 2015.

[37] M. Chafii, J. Palicot, and R. Gribonval, "Wavelet modulation: an alternative modulation with low energy consumption," *Comptes Rendus Physique*, vol. 18, no. 2, pp. 156–167, 2017.

[38] S. Linfoot, M. Ibrahim, and M. Al-akaidi, "Orthogonal wavelet division multiplex: an alternative to OFDM," *IEEE Transactions on Consumer Electronics*, vol. 53, no. 2, pp. 278–284, 2007.

[39] A. R. Lindsey, "Wavelet packet modulation for orthogonally multiplexed communication," *IEEE Transactions on Signal Processing*, vol. 45, no. 5, pp. 1336–1339, 1997.

[40] K. Kaur, *"Discrete wavelet transform based OFDM system using convolutional encoding,"* M.S. thesis, Thapar University, Patiala, India, 2014.

[41] S. Sheela, T. P. Surekha, and R. Arjun, "Analysis of BER in OFDM using wavelet and FFT based method," in *Proceedings of the International Conference on Current Trends in Computer, Electrical, Electronics and Communication (ICCT-CEEC)*, pp. 473–476, Mysore, India, September 2017.

[42] M. GovindaRaju and B. V. Uma, "Design and simulation of wavelet OFDM with wavelet denoising on AWGN channel," *International Journal of Advanced Research in Computer and Communication Engineering*, vol. 2, no. 8, pp. 3015–3018, 2013.

[43] K. Anitha, K. Dharmistan, and N. J. R. Muniraj, "Modified lifting based DWT/IDWT architecture for OFDM on virtex-5 FPGA," *Global Journal of Research in Engineering*, vol. 12, 2012.

[44] K. Abdullah and Z. M. Hussain, "Simulation of models and BER performances of DWT-OFDM versus FFT-OFDM," *Discrete Wavelet Transforms*, IntechOpen, London, UK, 2011.

[45] R. Kanti and M. RaiDr., "Comparative analysis of different wavelets in OWDM with OFDM for DVB-T," *International Journal of Advancements in Research & Technology*, vol. 2, no. 3, 2013.

[46] R. Bodhe, S. Joshi, and S. Narkhede, "Performance comparison of FFT and DWT based OFDM and selection of mother wavelet for OFDM," *International Journal of Computer Science and Information Technologies*, vol. 3, no. 3, pp. 3993–3997, 2012.

[47] G. Gowri, G. Uma Maheswari, E. Vishnupriya, S. Prabha, D. Meenakshi, and N. R. Raajan, "Performance analysis of DWTOFDM and FFT-OFDM systems," *International Journal of Engineering and Technology*, vol. 5, 2013.

[48] V. MB and M. N. S. Swamy, "Low power pipelined DWT-IDWT architecture for OFDM system on FPGA," *Procedia Engineering*, vol. 30, pp. 466–474, 2012.

[49] S. Mallat, *A Wavelet Tour of Signal Processing*, Academic Press, Cambridge, MA, USA, 1999.

[50] M. S. Chavan, N. Mastorakis, and M. Gaikwad, "in Proceedings of the Joint WSEAS International Conferences on Recent Researches in Communications," *Automation, Signal Processing, Nanotechnology, Astronomy and Nuclear Physics*, pp. 37–41, Cambridge, UK, 2011.

[51] G. Pajares and J. Manuel de la Cruz, *A Wavelet-Based Image Fusion Tutorial Pattern Recognition*, pp. 1855–1872, Elsevier, Amsterdam, Netherlands, 2004.

[52] T. S. Rappaport, G. R. MacCartney, M. K. Samimi, and S. Sun, "Wideband millimeter-wave propagation measurements and channel models for future wireless communication system design," *IEEE Transactions on Communications*, vol. 63, no. 9, pp. 3029–3056, 2015.

[53] E. F. James and P. Beatrice, "An overview on wavelets in source coding, communications, and networks," *EURASIP Journal on Image and Video Processing*, vol. 2007, no. 1, 2007.

[54] A. A. Zaidi, R. Baldemair, H. Tullberg et al., "Waveform and numerology to support 5G services and requirements," *IEEE Communications Magazine*, vol. 54, no. 11, pp. 90–98, 2016.